

## SYNTHETIC BIOLOGY

## A surface-display biohybrid approach to light-driven hydrogen production in air

Wei Wei,<sup>1,2</sup> Peiqing Sun,<sup>1</sup> Zhen Li,<sup>1,2</sup> Kuisong Song,<sup>1,2</sup> Wenyin Su,<sup>1,2</sup> Bao Wang,<sup>1,2</sup> Yangzhong Liu,<sup>3</sup> Jing Zhao<sup>1\*</sup>

Solar-to-chemical production by artificial and bioinspired photosynthetic systems is of tremendous interest to help solve current global energy and environmental problems. We developed a bioinorganic hybrid system for photocatalytic hydrogen production under aerobic conditions by combining light-harvesting semiconductors, hydrogenase catalysis, and self-aggregation of whole bacterial cells. We induced hydrogen production via self-photosynthesis in engineered *Escherichia coli* cells, which were originally designed for bioremediation, with in situ biosynthesis of biocompatible cadmium sulfide nanoparticles using a surface-display system. We also introduced a biomimetic silica encapsulation strategy into the engineered *E. coli* cells, enabling this hybrid system to continuously produce hydrogen for 96 hours, even under natural aerobic conditions. This biohybrid catalytic approach may serve as a general strategy for solar-to-chemical production.

## INTRODUCTION

The immoderate consumption of fossil fuels has caused many serious environmental problems, such as the greenhouse effect, global climate change, acid rain, and ozone depletion, which may greatly restrict the economic and social development of humans. The utilization of renewable and clean energy resources is highly desirable to address these global problems. Solar energy is the most important renewable energy resource on Earth, but it is difficult to harness. Thus, strategies exploiting the efficiency of photosynthesis for solar energy capture to enable the sustainable production of chemicals, such as hydrogen or other fuels, are urgently needed (1, 2). Using H<sub>2</sub> production as an example, several innovative inorganic-biological hybrid systems that combine the light-harvesting capabilities of photosystem I or a semiconductor and the catalytic power of the hydrogenase enzyme or a metal catalyst have been developed in the past two decades (3–5). Notably, King and colleagues (6–8) developed a series of highly efficient biohybrid hydrogen production systems by using CdTe nanocrystals/cadmium sulfide (CdS) nanorods and purified [Fe-Fe]-hydrogenase from *Clostridium acetobutylicum*. However, because of the oxygen-sensitive nature of these reactions, the low yield of the isolated hydrogenase, and the high cost of precious metals, the efficiency of photocatalytic H<sub>2</sub> production by these bioinorganic hybrid systems requires further improvement.

Whole bacterial cells have been used as biohybrid catalysts for H<sub>2</sub> production to overcome the limitations of both enzymes and synthetic catalysts in bioinorganic hybrid systems. Using this approach, several research groups have produced H<sub>2</sub> by hybridizing a titanium dioxide (TiO<sub>2</sub>) semiconductor with wild-type bacterial cells (9). Recently, the significant breakthrough reported by Honda *et al.* (10) showed that recombinant *Escherichia coli* cells expressing both hydrogenase and maturase genes enabled whole-cell photocatalytic H<sub>2</sub> production with TiO<sub>2</sub>. However, the low biocompatibility of semiconductors and the oxygen intolerance of hydrogenases limit the use of this whole-cell system for practical H<sub>2</sub> production.

Researchers have been working to optimize hybrid systems to protect the catalytic activity from oxygen stress and thus overcome these limitations. Notably, Douglas *et al.* (11) reported a smart self-assembling biomolecular catalyst for H<sub>2</sub> production using the bacteriophage P22 coat protein to encapsulate and protect the oxygen-tolerant [NiFe]-hydrogenase. Meanwhile, inspired by biomimetic mineralization, Tang *et al.* (12) developed a powerful silicification-induced green algae system for sustainable photobiological H<sub>2</sub> production under aerobic conditions. Inspired by these pioneering studies, we propose the development of an ideal whole-cell photocatalytic hydrogen production system that incorporates the following components: (i) a biocompatible light-harvesting inorganic semiconductor, (ii) active engineered *E. coli* cells as a biocatalyst, and (iii) a reliable shell to protect the reaction from oxygen. Here, we aim to develop engineered *E. coli* cells that combine the biosynthetic capability of CdS nanoparticles with surface-displayed heavy metal-binding proteins and the biocatalysis of oxygen-tolerant [NiFe]-hydrogenase. Combined with the biomimetic silicon encapsulation of whole *E. coli* cells, the bioinorganic hybrid system achieves photocatalytic hydrogen production under aerobic conditions (Fig. 1).

## RESULTS

## Biosynthesis of CdS nanoparticles

We began by exploring the biosynthesis of CdS nanoparticles by engineered *E. coli* cells. CdS is a well-studied semiconductor, and its photocatalytic activity has been thoroughly validated in bioinorganic hybrid systems (7, 13, 14). However, the synthesis of this semiconductor requires a complicated process and expensive reagents. The biocompatibility of the added exogenous metal materials also influences the efficiency of the biotic reactor (15). Yang *et al.* (16) achieved pivotal progress by pioneering a hybrid strategy for the photosynthesis of acetic acid from carbon dioxide using the nonphotosynthetic bacterium *Moorella thermoacetica*, which exhibits a unique metabolic pathway for biologically precipitated CdS nanoparticles. Inspired by the study of Yang and colleagues (17, 18), we realized that our previously engineered *E. coli* cells, which display a lead-specific binding protein PbrR on their surface, may perform a similar function as *M. thermoacetica*. The PbrR protein contains three conserved cysteine residues that coordinate the Pb(II) metal center through a unique hemi-directed geometry. The display of the PbrR protein on the *E. coli* cell surface permits the selective adsorption of both lead and cadmium ions

<sup>1</sup>State Key Laboratory of Coordination Chemistry, Institute of Chemistry and BioMedical Sciences, School of Chemistry and Chemical Engineering, Nanjing University, Nanjing 210093, China. <sup>2</sup>State Key Laboratory of Pharmaceutical Biotechnology, School of Life Sciences, Nanjing University, Nanjing 210093, China. <sup>3</sup>Chinese Academy of Sciences (CAS) Key Laboratory of Soft Matter Chemistry, CAS High Magnetic Field Laboratory, Department of Chemistry, University of Science and Technology of China, Hefei, China. \*Corresponding author. Email: jingzhao@nju.edu.cn

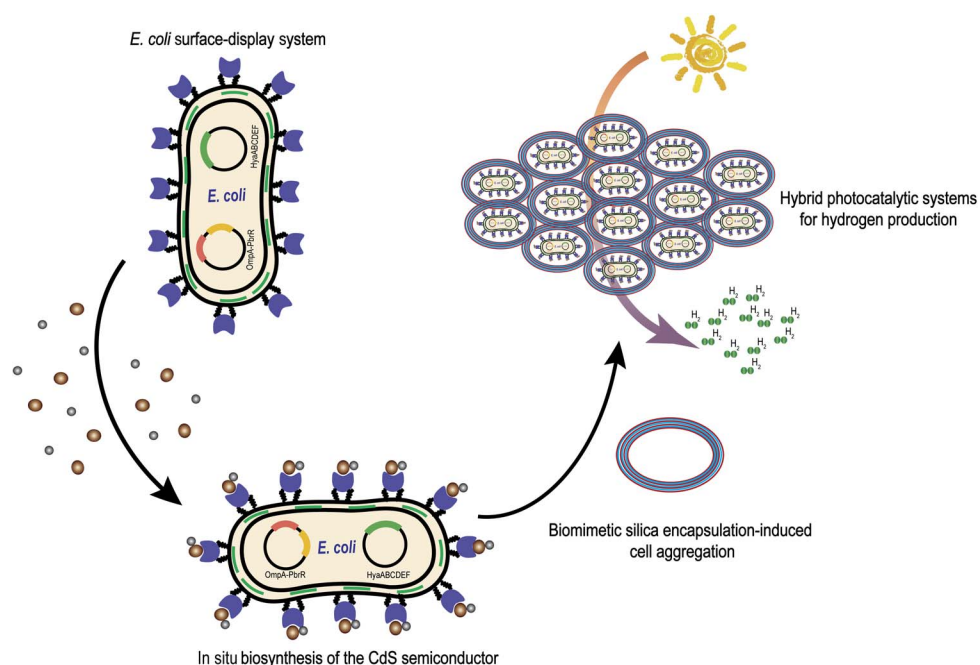


**Fig. 1. Proposed surface-display biohybrid approach to light-driven hydrogen production in air.**

and formed PbS and CdS nanoparticles on the outer membrane of the cells (19). Moreover, as the most important microorganism used for genetic engineering, *E. coli* has been well-studied in terms of its genomic and metabolic mechanisms and has become the most important cellular chassis in synthetic biology. Thus, the application of photosynthetic biohybrid systems to *E. coli* cells is highly desirable, thus expanding the scope of their applications.

Subsequently, we studied *E. coli* cells displaying PbrR on their surfaces for use in the biological precipitation of CdS nanoparticles. The fusion protein expression plasmid including *E. coli* outer membrane protein A (OmpA) and the PbrR protein, which was constructed as described in a previous study (19), was transformed into *E. coli* strain BL21 (Fig. 2A). The expression of the surface-displayed PbrR protein was induced with arabinose, and the biological precipitation of CdS nanoparticles was triggered by adding Cd<sup>2+</sup> to the culture medium. We used transmission electron microscopy with energy-dispersive x-ray spectroscopy (TEM-EDX) to observe the precipitation of the CdS nanoparticles. As shown in the TEM images, cadmium ions accumulated on the cell surface and formed uniform nanoparticle clusters <50 nm in size (Fig. 2B), which was also observed in the study of the *M. thermoacetica*-CdS hybrid system by Yang *et al.* (16). Furthermore, the EDX analysis of a randomly chosen area encompassing a portion of the CdS nanoparticles confirmed the elemental composition (Fig. 2C). The amount of biosynthesized CdS nanoparticles on the PbrR-overexpressing *E. coli* cell surface was measured using inductively coupled plasma mass spectrometry (ICP-MS) and reached  $8.09 \pm 0.70 \mu\text{g}/10^8$  cells after 24 hours (fig. S1), a value that was much higher than that on cells that were not displaying PbrR (19). These data confirmed the surface-displayed PbrR-mediated biological precipitation of CdS nanoparticles on the outer membranes of the cells.

### Hydrogen photosynthesis by the *E. coli* cell-CdS hybrid system

We performed ultraviolet-visible (UV-vis) spectral measurements to directly determine the optical band gap energy of these CdS nanoparticles and the photocatalytic capability for the biological precipitation of CdS

nanoparticles on the outer membranes of the bacterial cells (7, 14, 16). The lowest-energy transition of the biosynthesized CdS nanoparticles was detected in the visible region of the solar spectrum ( $E_g = 2.92$  eV,  $\lambda_{\text{absorption}} = 424$  nm; fig. S2), confirming the photocatalytic ability of the in situ biosynthesized CdS nanoparticles. The reaction solution also contained ascorbic acid and methylviologen (MV<sup>2+</sup>). Ascorbic acid is commonly used as the sacrificial electron donor to regenerate CdS nanoparticles (7, 10, 14, 20). The redox dye MV<sup>2+</sup> is a well-established electron mediator. In combination with MV<sup>2+</sup>, the semiconductor/bacterial cell hybrid system easily served as a biocatalyst for H<sub>2</sub> photosynthesis (fig. S3) (9, 10, 21). The concentrations of reduced MV in various experimental groups were measured under anaerobic conditions, confirming that the CdS nanoparticles precipitated on the engineered *E. coli* cells adsorb a photon of light and transfer an electron to MV<sup>2+</sup> (fig. S4). The amount of H<sub>2</sub> produced by this hybrid system under anaerobic conditions was detected using gas chromatography (GC). In the absence of light, trace amounts of H<sub>2</sub> were produced by the engineered *E. coli* cells in the presence or absence of CdS due to the anaerobic fermentation mediated by the endogenously expressed hydrogenase (22, 23). However, under illumination with a 350-W Xe lamp, the engineered *E. coli* cells ( $1 \times 10^8$ ) carrying CdS nanoparticles formed nearly  $13.40 \pm 1.20 \mu\text{mol H}_2$  after 6 hours and up to  $81.80 \pm 7.39 \mu\text{mol}$  after 24 hours, a value that was significantly higher than the values of the other treatments (Fig. 2D). In addition, the rate of H<sub>2</sub> photosynthesis in this hybrid system increased steadily from 0.56 to  $1.15 \mu\text{mol}/10^8$  cells per hour in the first 18 hours and then began to decrease due to bacterial death (Fig. 2E). On the basis of these results, H<sub>2</sub> production by our engineered *E. coli* cell-CdS hybrid system under anaerobic conditions was directly related to the biosynthesized CdS semiconductors and the activity of the whole-cell biocatalyst.

### Biomimetic silica encapsulation of the hybrid system

We next aimed to generate the semiconductor-*E. coli* cell hybrid system under aerobic conditions for more convenient applications.

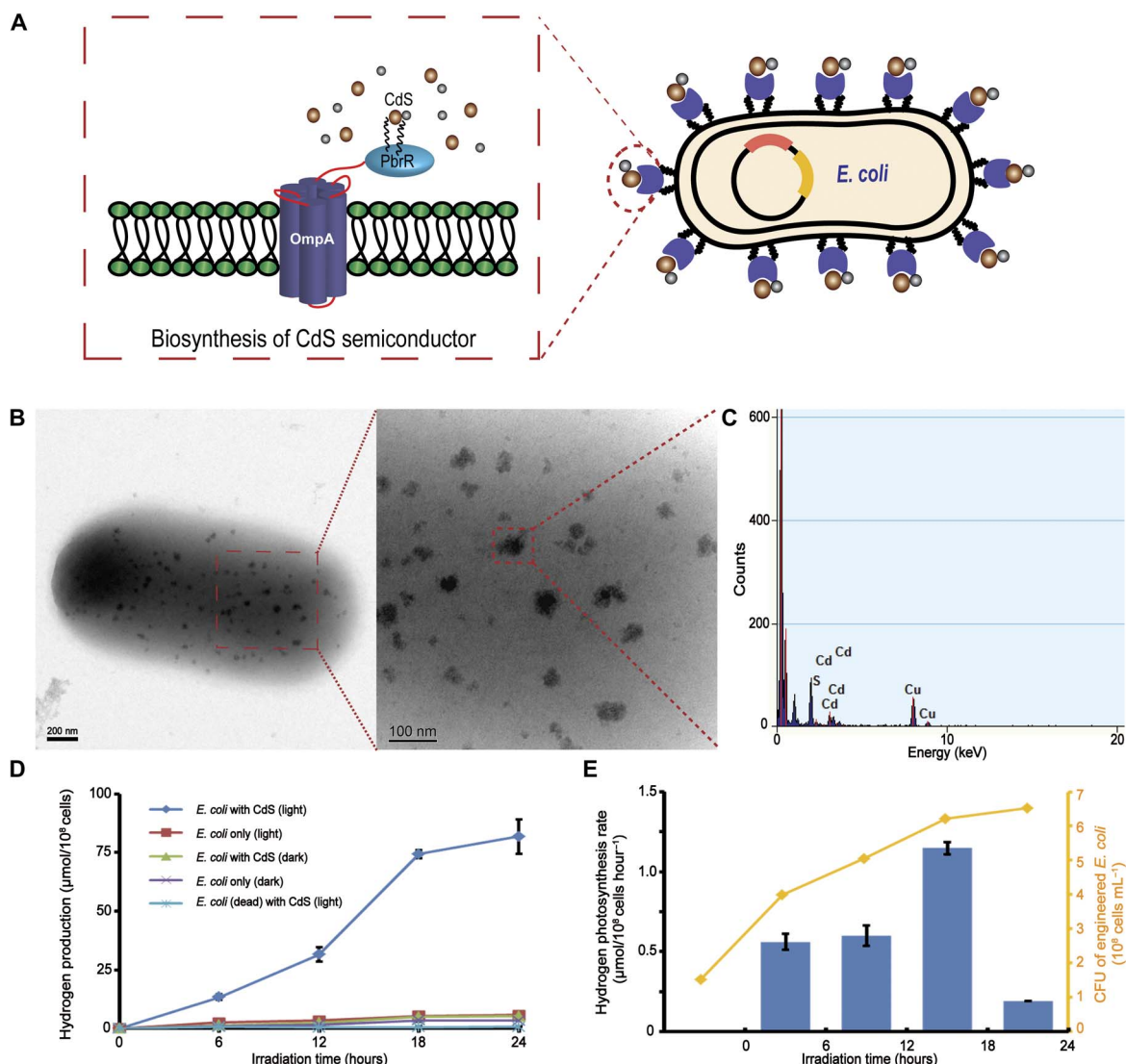


**Fig. 2. Hydrogen photosynthesis by the *E. coli* cell-CdS hybrid system.** (A) Detailed diagram of an engineered *E. coli* cell. (B) TEM images of biosynthesized CdS nanoparticles on the surface of an engineered *E. coli* cell. (C) EDX confirmation of randomly chosen CdS nanoparticle. (D) H<sub>2</sub> production by the hybrid system under anaerobic conditions. (E) Changes in the rate of H<sub>2</sub> production by the hybrid system during irradiation. SDs represent the averages of three independent experiments. CFU, colony-forming units.

Some living organisms have developed specific mineral structures that provide extra protection and unique functions through biomimetic mineralization (24, 25). Recently, biomimetic silica encapsulation based on layer-by-layer (LbL) assembly was successfully used for the cell surface modifications of living organisms such as yeast, algae, and bacteria (12, 26–28). Inspired by these pioneering studies, we introduced this cell encapsulation strategy into our semiconductor-*E. coli* hybrid system for hydrogen production in air. Using the reported LbL self-assembly method, we coated *E. coli* cells with cationic polyelectrolyte poly(diallyldimethylammonium chloride) (PDADMAC) and anionic polyelectrolyte sodium polystyrene sulfonate (PSS). The biomimetic silica-encapsulated cells were formed by placing surface-coated cells into a medium containing 50 mM silicic acid (26). According to Tang *et al.* (12), the cell aggregation induced by silica encapsulation leads to a specific phenomenon termed spatial-functional differentiation (SFD).

Upon SFD, cells in the shell and the mantle layer of the aggregate gradually consume oxygen through aerobic respiration, producing an anaerobic environment for the *E. coli* cells in the core. Consequently, the cells in the core are forced to undergo anaerobic metabolism, which protects the catalytic activity of the expressed hydrogenase (Fig. 3A). We used O<sub>2</sub> microsensors to examine the interior environment and confirm the microstructural features of our encapsulated *E. coli* aggregates (Fig. 3B). In the 2000-μm aggregates, the O<sub>2</sub> concentration decreased as the probe depth increased due to cell aggregation and aerobic metabolism. In the core of the aggregates, the O<sub>2</sub> concentration was approximately zero, suggesting that overexpressed hydrogenase was activated to produce hydrogen (Fig. 3B). The scanning electron microscopy (SEM) images also show a visual representation of the encapsulated *E. coli* aggregates (Fig. 3, C and D). The encapsulation essentially involves the dehydration of silicic acid, which mineralizes into

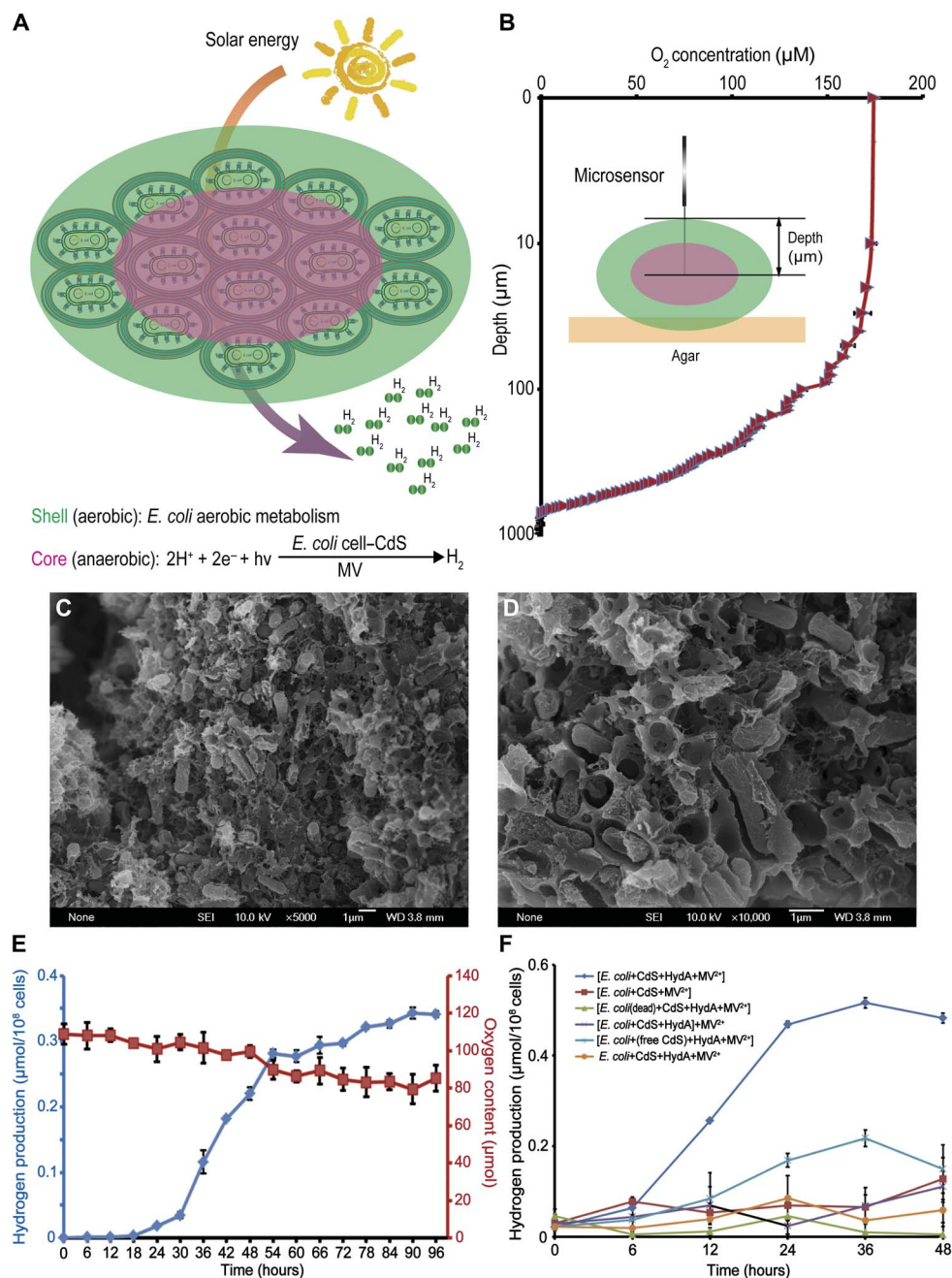


**Fig. 3. Light-driven hydrogen production by the encapsulated hybrid system in air.** (A) SFD in the semiconductor-engineered *E. coli* hybrid system encapsulated by biomimetic polymers. (B) Microsensor-based measurement of  $\text{O}_2$  concentration in the various independent encapsulated cell aggregates ( $n = 3$ ). (C and D) SEM images of encapsulated cell aggregates at different magnification. (E) Measurements of continuous hydrogen production in our biohybrid system. (F) Measurements of the amount of hydrogen produced by the various biohybrid systems under aerobic conditions ([ ] indicates silicification-induced aggregation). HydA, [NiFe]-hydrogenase HyaABCDEF.

silicon dioxide and acts as a glue to aggregate single *E. coli* cells into microspheres.

### Light-driven hydrogen production in air

Finally, we measured the amount of  $\text{H}_2$  produced by the encapsulated hybrid system under aerobic conditions. Because of the intrinsic oxygen sensitivity of *E. coli* hydrogenase, we transformed the [NiFe]-hydrogenase HyaABCDEF plasmid into the engineered *E. coli*. Protein expression was induced by adding isopropyl- $\beta$ -D-thiogalactoside (IPTG) after en-

capsulation. Hydrogen production by the hybrid system containing *E. coli*/CdS/hydrogenase/MV<sup>2+</sup> was monitored for 96 hours to test its ability to continuously produce hydrogen. We induced the expression of the surface-displayed PbrR protein and recombinant hydrogenase immediately after cell aggregation to extend the activities of the engineered *E. coli* cells. After the proteins were allowed to overexpress for 18 hours, we harvested the aggregates and resuspended them in a reaction solution containing 100 mM NaCl. Although  $94.98 \pm 5.27 \mu\text{mol}$  oxygen was present in the system,  $\text{H}_2$  production was significantly

increased at 18 hours and steadily increased over the next 72 hours to  $0.34 \pm 0.01 \mu\text{mol}/10^8$  cells (Fig. 3E).

The amount of  $\text{H}_2$  produced by different samples was detected using GC to examine the ability of encapsulation to protect the catalytic activity. As shown in Fig. 3F,  $\text{H}_2$  production was significantly increased 6 hours after hydrogenase overexpression in the encapsulated hybrid system under aerobic conditions.  $\text{H}_2$  production steadily increased and reached  $0.52 \pm 0.01 \mu\text{mol}/10^8$  cells at 36 hours. In contrast,  $\text{H}_2$  production was not detected in the samples without silica encapsulation, indicating that encapsulation is required for  $\text{H}_2$  production under aerobic conditions. Meanwhile, the amount of  $\text{H}_2$  produced by hybrid samples in which *E. coli* cells were inactivated or hydrogenase expression was not induced was also analyzed. The catalytic activity of  $\text{O}_2$ -intolerant hydrogenase experienced the greatest benefit from silicification-induced cell aggregation.

We measured hydrogen production in hybrid systems supplemented with  $\text{MV}^{2+}$  after cell encapsulation under aerobic conditions to probe whether the reduced MV is protected from  $\text{O}_2$  in the aggregates. If  $\text{MV}^{2+}$  was added after cell encapsulation and exposed to aerobic conditions during the reaction, then the hybrid system produced almost no hydrogen (Fig. 3F). Thus, both hydrogenase and  $\text{MV}^{2+}$  were protected from oxygen in the aggregates.

We added the same amount of free CdS nanoparticles to the reaction mixture, instead of the in situ biosynthesized CdS nanoparticles, under aerobic conditions to determine the photocatalytic activity of the free CdS nanoparticles in our biohybrid system. The system containing free CdS nanoparticles produced  $0.22 \pm 0.02 \mu\text{mol H}_2/10^8$  cells, implying a lower catalytic efficiency than in situ biosynthesized CdS nanoparticles.

## DISCUSSION

Efficient solar-to-chemical conversion strategies are greatly needed to address global energy and environmental problems. One important challenge is the development of simple and practical photosynthetic systems for the production of hydrogen or other fuels by exploring the fundamental chemistry of photosynthesis. Here, we developed a photocatalytic hydrogen biosynthesis strategy based on a semiconductor-engineered *E. coli* biohybrid system encapsulated with biomimetic polymers that function under aerobic conditions. Unlike reported microorganisms that induce nanoparticle precipitation through natural metabolic pathways, the surface-displaying bacterial system applied here facilitates the controllable biosynthesis of biocompatible CdS semiconductors by the model organism *E. coli* under mild conditions. In addition, our results further verified the light-harvesting capability of biosynthesized CdS semiconductors. This strategy could be applied to another well-established biological chassis, such as *Bacillus* or yeast, to expand its applications. The self-aggregated *E. coli* cells protect the activity of an oxygen-intolerant enzyme, ensuring that the enzyme performs efficient biological whole-cell catalysis under simple and mild conditions in air. Together, this bioinorganic hybrid system based on bacterial surface display and biomimetic silica encapsulation technologies will likely become an alternative approach for the convenient utilization of solar energy.

## MATERIALS AND METHODS

### In vivo expression of hydrogenase

*E. coli* BL21 transformed with the expression plasmid pET28a/HyaABCDEF was cultured in LB medium supplemented with kanamycin

(50  $\mu\text{g}/\text{ml}$ ) at 37°C. When the optical density at 600 nm ( $\text{OD}_{600}$ ) reached 0.6, cultures were transferred to a Coy anaerobic chamber (Coy Laboratory Products Inc.) with 95%  $\text{N}_2$  and 5%  $\text{H}_2$  gas. During anaerobic growth, cultures were supplemented with a sterile solution containing 1 mM IPTG, 1 mM  $(\text{NH}_4)_2\text{Fe}(\text{SO}_4)_2$ , and 1 mM  $\text{NiCl}_2$  in LB medium (all v/v, 1:1000). Cultures were incubated at room temperature under anaerobic conditions for 12 hours, with stirring.

### Surface display of the PbrR protein and in situ synthesis of CdS nanoparticles

The construction of the OmpA expression plasmid and methods used to overexpress OmpA-PbrR fusion proteins were previously described by Zhao *et al.* (19). For the in situ synthesis of CdS nanoparticles, 100  $\mu\text{M}$  cadmium ions were added to LB medium during the induction of the expression of OmpA-PbrR fusion proteins. Then, sample cells were harvested from LB medium every 6 hours by centrifugation (4000 rpm for 10 min) and washed with a 100 mM NaCl solution at least three times before analysis. The number of cells in each sample was determined by monitoring the  $\text{OD}_{600}$ . The CdS-adsorbed cells were lyophilized and subjected to wet ashing. All samples were further analyzed using ICP-MS to measure the amount of biosynthesized CdS nanoparticles on the engineered *E. coli* cell surface. *E. coli* cells containing biosynthesized CdS nanoparticles were harvested after 12 hours of induction for the subsequent analysis of biohydrogen production to maintain the best activity.

### TEM-EDX analysis of CdS nanoparticles

All TEM images were recorded using a JEOL JEM-2100 electron microscope at an accelerating bias voltage of 200 kV. After cadmium ion adsorption, the engineered cells were dispersed in double-distilled  $\text{H}_2\text{O}$ . A thick carbon film (20 to 30 nm) on a copper grid was dipped into the solution for 1 s, dried under atmospheric conditions, and then examined using TEM. The elemental analysis was performed with the EDX system (EDAX, AMETEK) attached to the microscope.

### Characterization of biologically precipitated CdS nanoparticles

The photocatalytic  $\text{MV}^{2+}$  reduction assay was performed using a 10-mm quartz cuvette with a cap and a light source (350-W Xe lamp). *E. coli* cells containing biosynthesized CdS nanoparticles were harvested from LB medium by centrifugation (4000 rpm for 10 min). The reaction system consisted of the same amounts of different semiconductors [TiO<sub>2</sub> anatase (10) and synthesized free CdS nanoparticles (29)] and 3 ml of 100 mM tris-HCl (pH 7), 150 mM NaCl, 5% glycerol, 100 mM ascorbic acid, and 5 mM  $\text{MV}^{2+}$  in the quartz cuvette.  $\text{O}_2$  was removed by bubbling  $\text{N}_2$  into the solution for 30 min. The reaction was initiated by light irradiation and stopped by centrifugation and separation of *E. coli*-CdS nanoparticles from the MV buffer. The absorption spectra were immediately measured after centrifugation (1000g for 1 min). The amount of reduced  $\text{MV}^{2+}$  ( $\text{MV}^+$ ) that formed was calculated by monitoring the  $\text{OD}_{605}$  using the molar conversion coefficient  $\epsilon = 1.3 \times 10^4 \text{ M}^{-1} \text{ cm}^{-1}$ . The UV-vis spectra of the *E. coli*-CdS hybrids in the solution were also obtained. The conduction band energy of the photo-excited CdS was determined using the Nernst equation.

### Measurements of photocatalytic $\text{H}_2$ production

Photocatalytic  $\text{H}_2$  production was measured using an external light source (350-W Xe lamp). Under anaerobic conditions in an anaerobic chamber (Coy Laboratory Products Inc.), 20 ml of LB medium

containing 1 mM  $(\text{NH}_4)_2\text{Fe}(\text{SO}_4)_2$ , 1 mM  $\text{NiCl}_2$ , 100 mM ascorbic acid, and 5 mM  $\text{MV}^{2+}$ , and engineered *E. coli* cells were prepared in 100-ml serum bottles. The system was evacuated to remove the  $\text{N}_2$  and  $\text{H}_2$  from the glove box atmosphere. The in situ synthesis of CdS nanoparticles and overexpression of hydrogenase were successively induced by adding IPTG after the reaction was initiated. The amount of  $\text{H}_2$  produced was analyzed by GC after direct injection onto the gas sampler using a microsyringe. Samples were then injected into a gas chromatograph (Kejie GC5890C, with silica gel column and thermal conductivity detector sensor) equipped with a thermal conductivity detector for the simultaneous determination of the concentrations of  $\text{H}_2$ ,  $\text{O}_2$ , and  $\text{N}_2$ . For measurements under aerobic conditions, the reaction system prepared under anaerobic conditions was subjected to biomimetic silica encapsulation.

### Biomimetic silica encapsulation

The engineered *E. coli* cells containing CdS nanoparticles were collected by centrifugation and then subjected to the biomimetic silica encapsulation protocol described by Choi *et al.* (26). The engineered cells were alternately immersed in the PDADMAC solution and the PSS solution for 5 min per step. After the LbL process, multilayer-coated cells were placed in the 50 mM silicic acid solution. The encapsulated biohybrid aggregates were finally harvested by centrifugation and uniformly dispersed into 2000- $\mu\text{m}$  particles (fig. S5).

### Microsensor measurements

The  $\text{O}_2$  microsensor was an OX25 microsensor (Unisense) with a 25- $\mu\text{m}$  tip diameter. The  $\text{O}_2$  concentrations in the aggregated *E. coli* were detected by piercing the aggregates with the  $\text{O}_2$  microelectrodes. The freshly prepared aggregated *E. coli* cells were used for measurements of hydrogen production for at least 12 hours under aerobic conditions. Then, the aggregates were harvested from the reaction system. A single layer of aggregates was fixed on the agar substrate (1 weight % agar), and the step size of the micromanipulator was 1  $\mu\text{m}$  when the tips of the microsensors pierced the aggregates.

### SUPPLEMENTARY MATERIALS

Supplementary material for this article is available at <http://advances.sciencemag.org/cgi/content/full/4/2/eaap9253/DC1>

fig. S1. The amount of biosynthesized CdS nanoparticles on the engineered *E. coli* cell surface was measured by ICP-MS.

fig. S2. Characterization of biologically precipitated CdS nanoparticles on the outer membranes of *E. coli* cells.

fig. S3. Photon transfer by in situ biosynthesized CdS nanoparticles.

fig. S4. Quantitative comparison of the photoelectrical capacity of an in situ biosynthesized CdS nanoparticle.

fig. S5. Image of encapsulated hybrid aggregates.

### REFERENCES AND NOTES

- R. E. Blankenship, D. M. Tiede, J. Barber, G. W. Brudvig, G. Fleming, M. Ghirardi, M. R. Gunner, W. Junge, D. M. Kramer, A. Melis, T. A. Moore, C. C. Moser, D. G. Nocera, A. J. Nozik, D. R. Ort, W. W. Parson, R. C. Prince, R. T. Sayre, Comparing photosynthetic and photovoltaic efficiencies and recognizing the potential for improvement. *Science* **332**, 805–809 (2011).
- A. W. D. Larkum, Limitations and prospects of natural photosynthesis for bioenergy production. *Curr. Opin. Biotechnol.* **21**, 271–276 (2010).
- M. Ihara, H. Nishihara, K.-S. Yoon, O. Lenz, B. Friedrich, H. Nakamoto, K. Kojima, D. Honma, T. Kamachi, I. Okura, Light-driven hydrogen production by a hybrid complex of a [NiFe]-hydrogenase and the cyanobacterial photosystem I. *Photochem. Photobiol.* **82**, 676–682 (2006).
- E. Reisner, D. J. Powell, C. Cavazza, J. C. Fontecilla-Camps, F. A. Armstrong, Visible light-driven  $\text{H}_2$  production by hydrogenases attached to dye-sensitized  $\text{TiO}_2$  nanoparticles. *J. Am. Chem. Soc.* **131**, 18457–18466 (2009).

- L. M. Utschig, N. M. Dimitrijevic, O. G. Poluektov, S. D. Chemerisov, K. L. Mulfort, D. M. Tiede, Photocatalytic hydrogen production from noncovalent biohybrid photosystem I/Pt nanoparticle complexes. *J. Phys. Chem. Lett.* **2**, 236–241 (2011).
- K. A. Brown, S. Dayal, X. Ai, G. Rumbles, P. W. King, Controlled assembly of hydrogenase-CdTe nanocrystal hybrids for solar hydrogen production. *J. Am. Chem. Soc.* **132**, 9672–9680 (2010).
- K. A. Brown, M. B. Wilker, M. Boehm, G. Dukovic, P. W. King, Characterization of photochemical processes for  $\text{H}_2$  production by CdS nanorod-[FeFe] hydrogenase complexes. *J. Am. Chem. Soc.* **134**, 5627–5636 (2012).
- M. B. Wilker, K. E. Shinopoulos, K. A. Brown, D. W. Mulder, P. W. King, G. Dukovic, Electron transfer kinetics in CdS nanorod-[FeFe]-hydrogenase complexes and implications for photochemical  $\text{H}_2$  generation. *J. Am. Chem. Soc.* **136**, 4316–4324 (2014).
- K. Gurunathan, Photobiocatalytic production of hydrogen using sensitized  $\text{TiO}_2$ - $\text{MV}^{2+}$  system coupled *Rhodospseudomonas capsulata*. *J. Mol. Catal. A Chem.* **156**, 59–67 (2000).
- Y. Honda, H. Hagiwara, H. Ida, T. Ishihara, Application to photocatalytic  $\text{H}_2$  production of a whole-cell reaction by recombinant *Escherichia coli* cells expressing [FeFe]-hydrogenase and maturase genes. *Angew. Chem. Int. Ed.* **55**, 8045–8048 (2016).
- P. C. Jordan, D. P. Patterson, K. N. Saboda, E. J. Edwards, H. M. Miettinen, G. Basu, M. C. Thielges, T. Douglas, Self-assembling biomolecular catalysts for hydrogen production. *Nat. Chem.* **8**, 179–185 (2016).
- W. Xiong, X. Zhao, G. Zhu, C. Shao, Y. Li, W. Ma, X. Xu, R. Tang, Silicification-induced cell aggregation for the sustainable production of  $\text{H}_2$  under aerobic conditions. *Angew. Chem. Int. Ed.* **54**, 11961–11965 (2015).
- R. Vogel, P. Hoyer, H. Weller, Quantum-sized PbS, CdS,  $\text{Ag}_2\text{S}$ ,  $\text{Sb}_2\text{S}_3$ , and  $\text{Bi}_2\text{S}_3$  particles as sensitizers for various nanoporous wide-bandgap semiconductors. *J. Phys. Chem.* **98**, 3183–3188 (1994).
- K. A. Brown, D. F. Harris, M. B. Wilker, A. Rasmussen, N. Khadka, H. Hamby, S. Keable, G. Dukovic, J. W. Peters, L. C. Seefeldt, P. W. King, Light-driven dinitrogen reduction catalyzed by a CdS:nitrogenase MoFe protein biohybrid. *Science* **352**, 448–450 (2016).
- P. W. King, Designing interfaces of hydrogenase-nanomaterial hybrids for efficient solar conversion. *Biochim. Biophys. Acta* **1827**, 949–957 (2013).
- K. K. Sakimoto, A. B. Wong, P. Yang, Self-photosensitization of nonphotosynthetic bacteria for solar-to-chemical production. *Science* **351**, 74–77 (2016).
- P. R. Chen, E. C. Wasinger, J. Zhao, D. van der Lelie, L. X. Chen, C. He, Spectroscopic insights into lead(II) coordination by the selective lead(II)-binding protein PbrR691. *J. Am. Chem. Soc.* **129**, 12350–12351 (2007).
- S. Huang, X. Liu, D. Wang, W. Chen, Q. Hu, T. Wei, W. Zhou, J. Gan, H. Chen, Structural basis for the selective Pb(II) recognition of metalloregulatory protein PbrR691. *Inorg. Chem.* **55**, 12516–12519 (2016).
- W. Wei, X. Liu, P. Sun, X. Wang, H. Zhu, M. Hong, Z.-W. Mao, J. Zhao, Simple whole-cell biodetection and bioremediation of heavy metals based on an engineered lead-specific operon. *Environ. Sci. Technol.* **48**, 3363–3371 (2014).
- H. Borsook, G. Keighley, Oxidation-reduction potential of ascorbic acid (vitamin C). *Proc. Natl. Acad. Sci. U.S.A.* **19**, 875–878 (1933).
- M. Demuez, L. Cournac, O. Guerrini, P. Soucaille, L. Girbal, Complete activity profile of *Clostridium acetobutylicum* [FeFe]-hydrogenase and kinetic parameters for endogenous redox partners. *FEMS Microbiol. Lett.* **275**, 113–121 (2007).
- R. Nandi, S. Sengupta, Microbial production of hydrogen: An overview. *Crit. Rev. Microbiol.* **24**, 61–84 (1998).
- A. Trchounian, Mechanisms for hydrogen production by different bacteria during mixed-acid and photo-fermentation and perspectives of hydrogen production biotechnology. *Crit. Rev. Biotechnol.* **35**, 103–113 (2015).
- C. E. Hamm, R. Merkel, O. Springer, P. Jurkojc, C. Maier, K. Prechtel, V. Smetacek, Architecture and material properties of diatom shells provide effective mechanical protection. *Nature* **421**, 841–843 (2003).
- F. Nudelman, N. A. J. M. Sommerdijk, Biomimetalization as an inspiration for materials chemistry. *Angew. Chem. Int. Ed.* **51**, 6582–6596 (2012).
- S. H. Yang, K.-B. Lee, B. Kong, J.-H. Kim, H.-S. Kim, I. S. Choi, Biomimetic encapsulation of individual cells with silica. *Angew. Chem. Int. Ed.* **48**, 9160–9163 (2009).
- W. Chen, G. Wang, R. Tang, Nanomodification of living organisms by biomimetic mineralization. *Nano Res.* **7**, 1404–1428 (2014).
- W. Xiong, Z. Yang, H. Zhai, G. Wang, X. Xu, W. Ma, R. Tang, Alleviation of high light-induced photoinhibition in cyanobacteria by artificially conferred biosilica shells. *Chem. Commun.* **49**, 7525–7527 (2013).
- H. Yan, J. Yang, G. Ma, G. Wu, X. Zong, Z. Lei, J. Shi, C. Li, Visible-light-driven hydrogen production with extremely high quantum efficiency on Pt-PdS/CdS photocatalyst. *J. Catal.* **266**, 165–168 (2009).

### Acknowledgments

**Funding:** Financial support was provided by the National Science Foundation of China (nos. 21622103, 21571098, and 21671099), the Natural Science Foundation of Jiangsu Province (no. BK20160022), and the Fundamental Research Funds for the Central Universities

(nos. 020514380117 and 020814380002). **Author contributions:** W.W. and P.S. designed the experiments. W.W., P.S., Z.L., K.S., W.S., and B.W. performed the experiments. W.W., P.S., Z.L., Y.L., and J.Z. wrote the manuscript, and J.Z. and W.W. supervised the research.

**Competing interests:** The authors declare that they have no competing interests.

**Data and materials availability:** All data needed to evaluate the conclusions in the paper are present in the paper and/or the Supplementary Materials. Additional data related to this paper may be requested from the authors.

Submitted 11 September 2017

Accepted 23 January 2018

Published 21 February 2018

10.1126/sciadv.aap9253

**Citation:** W. Wei, P. Sun, Z. Li, K. Song, W. Su, B. Wang, Y. Liu, J. Zhao, A surface-display biohybrid approach to light-driven hydrogen production in air. *Sci. Adv.* **4**, eaap9253 (2018).

## A surface-display biohybrid approach to light-driven hydrogen production in air

Wei Wei, Peiqing Sun, Zhen Li, Kuisong Song, Wenyin Su, Bao Wang, Yangzhong Liu and Jing Zhao

*Sci Adv* 4 (2), eaap9253.

DOI: 10.1126/sciadv.aap9253

### ARTICLE TOOLS

<http://advances.sciencemag.org/content/4/2/eaap9253>

### SUPPLEMENTARY MATERIALS

<http://advances.sciencemag.org/content/suppl/2018/02/16/4.2.eaap9253.DC1>

### REFERENCES

This article cites 29 articles, 4 of which you can access for free  
<http://advances.sciencemag.org/content/4/2/eaap9253#BIBL>

### PERMISSIONS

<http://www.sciencemag.org/help/reprints-and-permissions>

Use of this article is subject to the [Terms of Service](#)

---

*Science Advances* (ISSN 2375-2548) is published by the American Association for the Advancement of Science, 1200 New York Avenue NW, Washington, DC 20005. 2017 © The Authors, some rights reserved; exclusive licensee American Association for the Advancement of Science. No claim to original U.S. Government Works. The title *Science Advances* is a registered trademark of AAAS.